$B_s \to D_s^{(*)}$ form factors from lattice QCD with $N_f = 2$ Wilson-clover quarks

Benoît Blossier,[a] Pierre Henri Cahue,[b] Jochen Heitger,[c] Simone La Cesa,[b] Jan Neuendorf[a,c,*] and Savvas Zafeiropoulos[d]

[a]*Laboratoire de Physique des 2 Infinis Irène Joliot-Curie, CNRS/IN2P3, Université Paris-Saclay, Bâtiment 210, 91405 Orsay Cedex, France*

[b]*Laboratoire de Physique Subatomique et de Cosmologie, CNRS/IN2P3, 53 Avenue des Martyrs, 38000 Grenoble, France*

[c]*Institut für Theoretische Physik, Westfälische Wilhelms-Universität Münster, Wilhelm-Klemm-Str. 9, 48149 Münster, Germany*

[d]*Aix Marseille Univ, Université de Toulon, CNRS, CPT, Marseille, France*

E-mail: blossier@ijclab.in2p3.fr, cahue@lpsc.in2p3.fr, heitger@wwu.de, simo.lcs@gmail.com, jan.neuendorf@wwu.de, savvas.zafeiropoulos@cpt.univ-mrs.fr

We report on a two-flavour lattice QCD determination of the $B_s \to D_s$ and $B_s \to D_s^*$ transitions, which in the heavy quark limit can be parameterised by the form factors $\mathcal{G}$, and h_{A_1}, h_{A_2} and h_{A_3}. In the search of New Physics through tests of lepton-flavour universality, B_s decay channels are complementary to B decays and widely studied at B factories and LHCb. The purpose of our study is to explore a suitable method to extract form factors associated with $b \to c$ currents from lattice QCD. In particular, we present numerical results for $\mathcal{G}$ and h_{A_1}.

The 38th International Symposium on Lattice Field Theory, LATTICE2021 26th-30th July, 2021
*Zoom/Gather@Massachusetts Institute of Technology*

---

*Speaker

1. Motivation and preliminary remarks

The purpose of this work is to study whether Wilson-Clover fermions, in combination with the step-scaling in mass method [1, 2], allow for the extraction of reliable results for B decays, as far as cut-off effects and contamination by excited states are concerned. We perform an analysis on $N_f = 2$ ensembles, created by the CLS effort. The work presented here is described in more detail in the corresponding article [3].

We consider the semi leptonic decay B_s to $D_s^{(*)}$, as sketched in fig. 1.
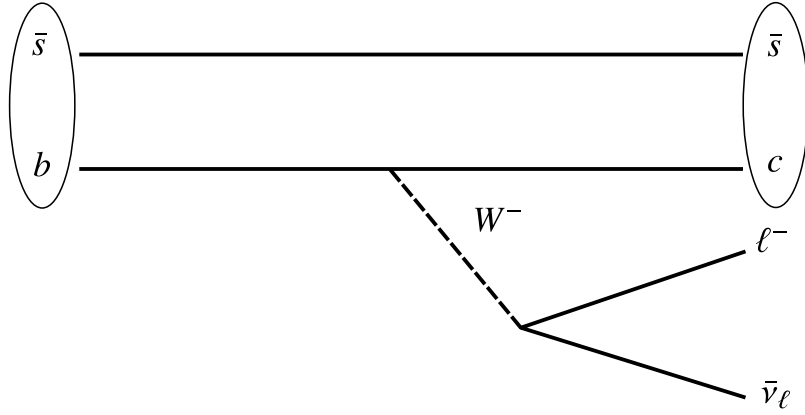
Figure 1: Schematic of the decay $\bar{B}_s^0 \rightarrow D_s^{+(*)} \ell^- \bar{\nu}_\ell$

The decay width includes the CKM matrix element V_{cb} as well as a form factor that encodes the long-distance dynamics of QCD. Our main focus is on $B_s \rightarrow D_s$, where this factor is called $\mathcal{G}$.

$$\frac{d\Gamma_{B_s \rightarrow D_s}}{dw} \propto |V_{cb}|^2 \cdot |\mathcal{G}(w)|^2 \cdot G_F^2 (m_{B_s} + m_{D_s})^2, \tag{1}$$

where $w = \frac{E_{D_s}}{m_{D_s}}$ is the relative velocity of the $D_s^{(*)}$ meson. It is h_{A_1} for $B_s \rightarrow D_s^*$.

The strong contribution only depends on w. It is suitable to describe physics of heavy-light mesons by means of Heavy Quark Effective Theory (HQET). In first approximation, the light degrees of freedom live in the potential created by a static source of colour. We are interested in the zero recoil case, where $w = 1$. In the heavy quark limit, Heavy Quark Symmetry implies that $\mathcal{G}^{m_h \rightarrow \infty}(1) = 1$. Since b and c are heavy, we can predict ab initio that $\mathcal{G}(1)$ is close to one.

The decay can be parametrised as

$$\langle D_s(k)|\bar{b}\gamma_\mu c|B_s(p)\rangle = A_\mu(p, k)\mathcal{G}(w) + B_\mu(p, k)f_0(w), \tag{2}$$

where all dependencies other than the momentum transfer have been absorbed. The left hand side is a matrix element, which can be accessed on the lattice [2].
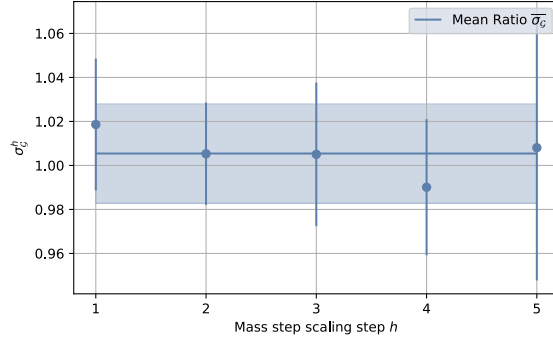
Figure 2: Ratios σ at the different mass step-scaling steps.

2. Mass step-scaling

To control cut-off effects we have decided not to compute our observables directly at the b-quark scale. Instead, on each ensemble, a set of six meson masses $m_{h_{i\in[0,..,5]}s}$ is chosen to fulfill,

$$m_{h_0 s} = m_{D_s}, \tag{3}$$

$$\frac{m_{h_{i+1}s}}{m_{h_i s}} = \lambda \quad \text{with} \quad \lambda = \sqrt[6]{\frac{m_{B_s}}{m_{D_s}}}. \tag{4}$$

The bare heavy quark mass is tuned to ensure these relations.

This approach has more advantages than just allowing us to extrapolate our results to the B_s mass. As mentioned in the previous section, $\mathcal{G}(w = 1)$ equals one at the elastic point $m_{h_0 s} = m_{D_s}$. We exploit this, by expressing $\mathcal{G}^{B_s \rightarrow D_s}(w = 1)$ as:

$$\mathcal{G}^{B_s \rightarrow D_s}(w = 1) = \mathcal{G}_{i=6}(1) = \frac{\mathcal{G}_6(1)}{\mathcal{G}_5(1)} \cdot \frac{\mathcal{G}_5(1)}{\mathcal{G}_4(1)} \cdot ... \cdot \frac{\mathcal{G}_1(1)}{\mathcal{G}_0(1)} \cdot \mathcal{G}_0(1) \tag{5}$$

$$= \sigma_6 \cdot \sigma_5 \cdot ... \cdot \sigma_1 \quad \text{with} \quad \sigma_i = \frac{\mathcal{G}_i(1)}{\mathcal{G}_{i-1}(1)} \tag{6}$$

We only need to consider the ratios of $\mathcal{G}$'s, which leads to the cancellation of correlated errors and renormalization constants. But since we do not compute $\mathcal{G}_6$, we do not get a value for σ_6 either. This means that we have to perform some extrapolation to gain access to it. In Fig. 2 we show that our ratios are compatible with a constant. Therefore, for our final results in section 5, we opted for computing our final result from the mean value $\bar{\sigma}$ as $\mathcal{G}^{B_s \rightarrow D_s}(w = 1) = \bar{\sigma}^6$.

For the computation of h_{A_1} we can gain no such advantage, since $h_{A_1}{}^{D_s^* \rightarrow D_s} \neq 1$. Nevertheless, we use the same approach for consistency.

3. Matrix elements

Looking at the left hand side of eq. (2), we can see the form $\langle P|V|P \rangle$. On the lattice, we compute a corresponding three-point correlation function:

$$C_{ij}^\theta(\tfrac{T}{2}], t) = \sum_{\vec{x}, \vec{y}} \langle P_{hs, i}(\tfrac{T}{2}) V_{hc, \mu}^{I, \theta}(t) P_{cs, j}^{\dagger \theta}(0) \rangle$$

$$\overset{1 \ll t \ll \frac{T}{2}}{\sim} \frac{Z_{H_s} Z_{D_s}}{4 E_{H_s} E_{D_s}} e^{-E_{H_s} t} e^{-E_{D_s} (\frac{T}{2} - t)} \langle D_s(k) | \bar{b} \gamma_\mu c | H_s(p) \rangle, \tag{7}$$

where Z is the source amplitude. The bare matrix element at the left hand side of eq. (2) appears. The source-sink-separation is kept constant at $\frac{T}{2}$, which is $\gtrsim 2\,\text{fm}$ for the studied ensembles.

Using the two point correlators belonging to the propagation of H_s and $D_s^{(*)}$, we can extract the energies and amplitudes and eliminate them from eq. (7).

To optimise for a better overlap with the respective ground states of $D_s^{(*)}$ and H_s, we made use of multiple smeared sources and sinks and the generalised eigenvalue problem (GEVP). The (ground state) eigenvectors were computed for the two point correlators. They could then also be used to project the three-point correlator (eq. (7)), since the setup of the sources is consistent.

4. Lattice details

Our data were computed on eight different CLS ensembles with $N_f = 2$ and $O(a)$ improved Wilson-Clover fermions [4, 5].
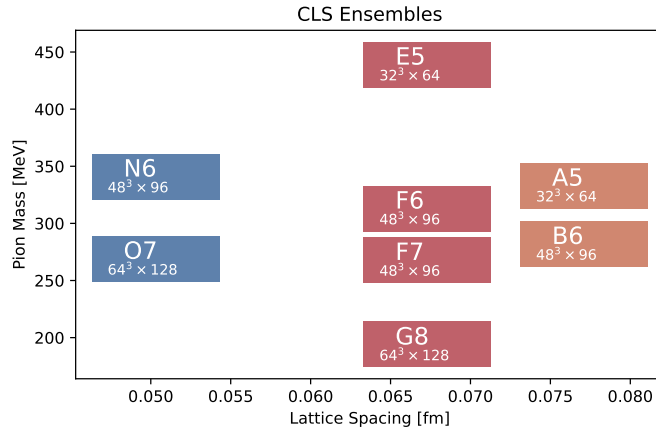

Figure 3: Parameters of the used CLS ensembles.

The parameters of these ensembles are shown in Fig. 3. Hopping-parameters corresponding to c- and s-quarks, as well as the appropriately tuned values for the mass step-scaling steps are known from previous works [6, 7].

We are interested in the case of zero recoil ($w = 1$). The kinematic vanishing of the spatial matrix element $\langle D_s | V^i | B_s \rangle$ makes it impossible to extract $\mathcal{G}$ at $w = 1$ directly. For h_{A_1} we do not have this problem. We need to calculate $\mathcal{G}$ with different momentum transfers and extrapolate
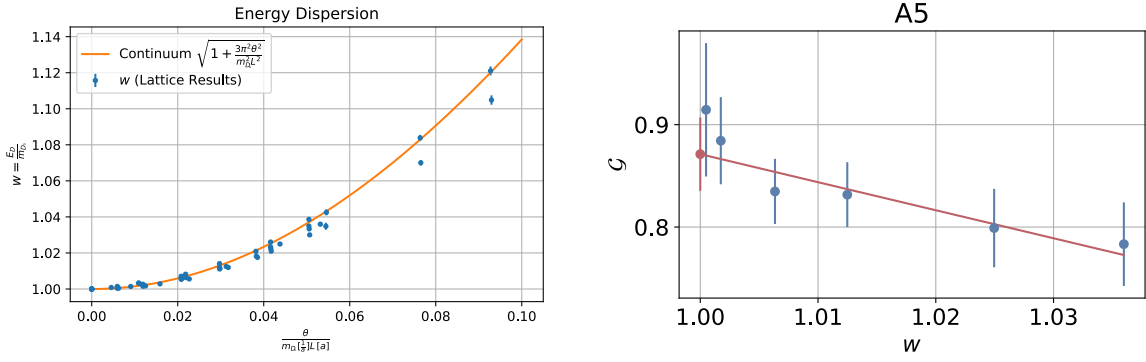
Figure 4: (*left*) Dispersion relation for D_s with twisted boundary conditions. (*right*) Exemplary extrapolation of $\mathcal{G}$ to $w = 1$.
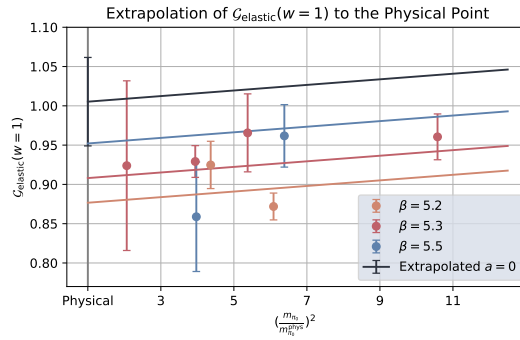
Figure 5: Visualisation of the combined fit eq. (8) and extrapolation to the physical point for $\mathcal{G}_{\text{elastic}}$.

to zero recoil. To introduce momenta to the D_s, we impose spatial isotropic twisted-boundary conditions with a twisting angle θ to the c-quark. On each ensemble we compute the correlators for six values of θ as well as without twisting. In Fig. 4 we see that the introduction of a spatial twisting-angle for the c-quark does indeed inject the B_s with the expected momentum. Here $w = \frac{E_{D_s}}{m_{D_s}}$ is computed directly from the spectroscopy of the two point correlation functions. We obtain $\mathcal{G}$ for all values of θ and perform a linear extrapolation in $(w - 1)$. An example for this is shown in Fig. 4.

5. Results at the physical point

For all observables o, which need to be extrapolated in this section, we use the following ansatz:

$$o(a, m_\pi^2) = o_0 + o_1 \times (m_\pi^2 / m_\pi^{2,\text{physical}}) + o_2 \times (a/a_{\beta=5.3})^2 \qquad (8)$$

$$\implies o^{\text{physical}} = o(0, m_\pi^{2,\text{physical}}) = o_0 + o_1 \qquad (9)$$

For some quantities, other parameters such as heavy mass dependency and a dependency on a possible mistuning of the mass step-scaling steps has been tried as well [3].

We have asserted that $\mathcal{G}(1)$ is equal to one at the elastic point. This can be shown from the lattice data by performing an extrapolation to the physical point. The result of this extrapolation is
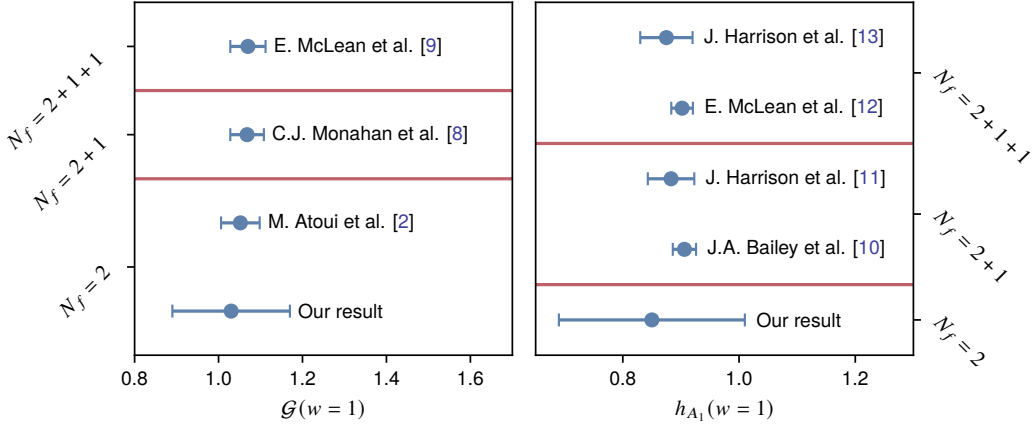
Figure 6: Comparison to previous results for $\mathcal{G}$ (*left*) and h_{A_1} (*right*).

shown in Fig. 5. It is indeed compatible with one.

In the case of $\mathcal{G}$ we only need to consider the ratios between successive mass step-scaling steps. These are computed directly on every ensemble to ensure the cancellation of correlated errors. Then the ratios are extrapolated (separately for every mass step-scaling step) to the physical point according to eq. (8). A combined fit with additional parameters has been tried as well with compatible results. The resulting ratios at the physical point are shown in Fig. 2.

We get a final result for $\mathcal{G}$:

$$\mathcal{G}^{B_s \rightarrow D_s}(w = 1) = \prod_{i=1}^{6} \sigma_i \approx \overline{\sigma}^6 = 1.03(14) \tag{10}$$

For h_{A_1} we obtain

$$h_{A_1}^{B_s \rightarrow D_s^*}(1) = h_{A_1}^{D_s \rightarrow D_s^*}(1) \times \prod_{i=1}^{6} \sigma_i^{h_{A_1}} \approx h_{A_1}^{D_s \rightarrow D_s^*}(1) \times (\overline{\sigma^{h_{A_1}}})^6 \tag{11}$$

$$= 0.825(83) \times (1.005(23))^6 = 0.85(16). \tag{12}$$

6. Discussion and conclusion

In this exploratory $N_f = 2$ study, we have obtained the form factors $\mathcal{G}(w = 1) = 1.03(14)$ and $h_{A_1}(w = 1) = 0.86(16)$, associated with the semileptonic decays $B_s \rightarrow D_s$ and $B_s \rightarrow D_s^*$ respectively, using the method of step-scaling in mass.

From Fig. 6, where we show a comparison to previous results, one infers that we are facing substantial statistical uncertainty. This might in part be explained by the large source-sink-separation. Moreover, the mass step scaling method itself has, of course, a significant impact on the error of the final result, since the ratios are all multiplied in the end. Most results, which were obtained by projecting with GEVP eigenvalues, are compatible with results obtained by using only the source with the largest gaussian smearing.

We also observed that small momenta injected by twisted-boundary conditions provide a stable extrapolation to the point of zero recoil.

Finally, as can be seen in Fig. 2, the data are not sensitive to the change in the heavy mass $M_{h_i s}$.

Acknowledgment

References

[1] (ETM), B. Blossier et al., *A Proposal for B-physics on current lattices*, *JHEP* **04** (2010) 049, [0909.3187].

[2] M. Atoui, D. Becirevic, V. Morénas and F. Sanfilippo, *Lattice QCD study of* $B_s \to D_s \ell \bar{\nu}_\ell$ *decay near zero recoil*, *PoS* **LATTICE2013** (2014) 384, [1311.5071].

[3] B. Blossier, P.-H. Cahue, J. Heitger, S. LaCesa, J. Neuendorf and S. Zafeiropoulos, *On the extraction of* $B_s \to D_s^{(*)}$ *form factors from* $N_f = 2$ *lattice QCD*, 2110.10061.

[4] B. Sheikholeslami and R. Wohlert, *Improved Continuum Limit Lattice Action for QCD with Wilson Fermions*, *Nucl. Phys. B* **259** (1985) 572.

[5] (ALPHA), M. Lüscher, S. Sint, R. Sommer, P. Weisz and U. Wolff, *Nonperturbative O(a) improvement of lattice QCD*, *Nucl. Phys. B* **491** (1997) 323–343, [hep-lat/9609035].

[6] (ALPHA), P. Fritzsch, F. Knechtli, B. Leder, M. Marinkovic, S. Schaefer, R. Sommer et al., *The strange quark mass and lambda parameter of two flavor qcd*, *Nuclear Physics B* **865** (Dec, 2012) 397–429.

[7] (ALPHA), J. Heitger, G. M. von Hippel, S. Schaefer and F. Virotta, *Charm quark mass and D-meson decay constants from two-flavour lattice QCD*, *PoS* **LATTICE2013** (2014) 475, [1312.7693].

[8] C. J. Monahan, H. Na, C. M. Bouchard, G. P. Lepage and J. Shigemitsu, $B_s \to D_s \ell \nu$ *Form Factors and the Fragmentation Fraction Ratio* f_s/f_d, *Phys. Rev. D* **95** (2017) 114506, [1703.09728].

[9] (HPQCD), E. McLean, C. T. H. Davies, J. Koponen and A. T. Lytle, $B_s \to D_s \ell \nu$ *Form Factors for the full* q^2 *range from Lattice QCD with non-perturbatively normalized currents*, *Phys. Rev. D* **101** (2020) 074513, [1906.00701].

[10] (Fermilab Lattice, MILC), J. A. Bailey et al., *Update of* $|V_{cb}|$ *from the* $\bar{B} \to D^* \ell \bar{\nu}$ *form factor at zero recoil with three-flavor lattice QCD*, *Phys. Rev. D* **89** (2014) 114504, [1403.0635].

[11] (HPQCD), J. Harrison, C. Davies and M. Wingate, *Lattice QCD calculation of the* $B_{(s)} \to D_{(s)}^* \ell \nu$ *form factors at zero recoil and implications for* $|V_{cb}|$, *Phys. Rev. D* **97** (2018) 054502, [1711.11013].

[12] (HPQCD), E. McLean, C. T. H. Davies, A. T. Lytle and J. Koponen, *Lattice QCD form factor for* $B_s \to D_s^* l \nu$ *at zero recoil with non-perturbative current renormalisation*, *Phys. Rev. D* **99** (2019) 114512, [1904.02046].

[13] (HPQCD), J. Harrison and C. T. H. Davies, $B_s \to D_s^*$ *Form Factors for the full* q^2 *range from Lattice QCD*, 2105.11433.

PoS(LATTICE2021)056